Journal of Macromolecular Science, Part A
Publication details, including instructions for authors and subscription information:
http://www.informaworld.com/smpp/title~content=t713597274

Synthesis of UV-Cured Silicone Resin/Silica Nanocomposites from UV-Curable Polysilisiquioxane and Methacrylate-Functionalized Silica

Limin Zang[a]; Jiahe Luo[a]; Jinshan Guo[a]
[a] Institute of Polymer Science and Engineering, College of Chemistry and Chemical Engineering, Lanzhou University, Gansu, China

Online publication date: 30 July 2010

To cite this Article Zang, Limin , Luo, Jiahe and Guo, Jinshan(2010) 'Synthesis of UV-Cured Silicone Resin/Silica Nanocomposites from UV-Curable Polysilisiquioxane and Methacrylate-Functionalized Silica', Journal of Macromolecular Science, Part A, 47: 9, 935 — 940
To link to this Article: DOI: 10.1080/10601325.2010.501666
URL: http://dx.doi.org/10.1080/10601325.2010.501666

Journal of Macromolecular Science, Part A: Pure and Applied Chemistry (2010) **47**, 935–940

ISSN: 1060-1325 print / 1520-5738 online
DOI: 10.1080/10601325.2010.501666

Synthesis of UV-Cured Silicone Resin/Silica Nanocomposites from UV-Curable Polysilisiquioxane and Methacrylate-Functionalized Silica

LIMIN ZANG, JIAHE LUO and JINSHAN GUO*

Institute of Polymer Science and Engineering, College of Chemistry and Chemical Engineering, Lanzhou University, Gansu, China

Received January 2010, Accepted April 2010

A series of silicone resin/silica polymeric nanocomposites with 0–6 wt% silica content, comprising well-distributed silica nanoparticles in silicone resin matrix, have been synthesized from a UV-curable polysilisiquioxane (UV-PSL) and a methacrylate-functionalized silica via UV-curing in the presence of 1-hydroxycyclohexyl phenyl ketone (Irgacure 184) as photoinitiator. To enhance the interfacial interaction, the silica surface was firstly treated with 3-(methacryloxy) propyl trimethoxysilane (MPTS), and its structure was analyzed by FTIR spectrophotometry. The thermal stability of nanocomposites was slightly enhanced with the addition of silica particles. SEM studies indicate that silica particles were dispersed homogenously through the polymer matrix. The physical and mechanical properties such as the thickness, hardness, adhesion, impact strength as well as gloss were examined.

Keywords: Silica particles, silicone resin, UV-curing, nanocomposite

1 Introduction

In the last 10 years, research activities have been immensely focused on the synthesis and characterization of polymeric nanocomposites because of their excellent performance compared to conventional composite materials (1–3). It has been reported that mechanical and thermo-mechanical property improvements are definitely higher in the case of nanosized with respect to micro-sized dispersed filler particles (4). Nanocomposites usually consist of nanosized inorganic particles (SiO_2 (5), TiO_2 (6), ZnO (7), magnetic oxides (8–10), and clay (11)) dispersed into a polymeric matrix. To obtain better compatibility between the filler and the host polymeric material, the surface modification of the inorganic nanoparticles by using acrylic/vinylic or epoxy functional trialkoxysilanes is recommended (12).

UV-curable nanocomposites, which combined the advantages of the UV-curing process and nanotechnology, can be used in fields such as coatings, printing, inks, and adhesives (13–16). Because of chemical bonds between organic and inorganic phase, materials performed good mechanical and physical properties. There were many reports on UV-curable nanocomposites containing clay (17–21) and nanosilica (15, 22, and 23). This method of producing polymer nanocomposites has been extended to different types of UV-curable resins such as epoxides and vinyl ethers (24, 25), as well as to other systems (26). In recent years, siloxane polymers which are viewed as inorganic-organic hybrid polymers (also known as polysiloxanes) have attracted great attention for their application in heat-resisting coatings owing to firstly, the high energy of the siloxane (Si–O–Si) bond, secondly, the oxidized nature of siloxane bond and thirdly, the high oxidation and temperature resistances of common side chain substitutions such as methyl or phenyl groups. In addition, very little work has been published on silicone based composites.

Here, we study the preparation of silicone resin containing well-dispersed nanosilica with improved thermal stability by UV-curable polymerization. The UV-curable polysilisiquioxane (UV-PSL) containing methacrylate groups can be polymerized by UV irradiation. To enhance the interfacial interaction in silica nanoparticles filled polymer composites, the surface of the silica particles was modified with 3-(methacryloxy) propyl trimethoxysilane (MPTS), and then polymer nanocomposite coatings with 0–6 wt% modified silica content were prepared by UV-induced polymerization (Sch. 1). Adhesion, gloss, and hardness tests were performed on tinplate panels coated with those

*Address correspondence to: Jinshan Guo, Institute of Polymer Science and Engineering, College of Chemistry and Chemical Engineering, Lanzhou University, Tianshui South Road 222, Gansu 730000, China. Tel: +86 931 8912516; Fax: +86 931 8912582; E-mail: gjs@lzu.edu.cn

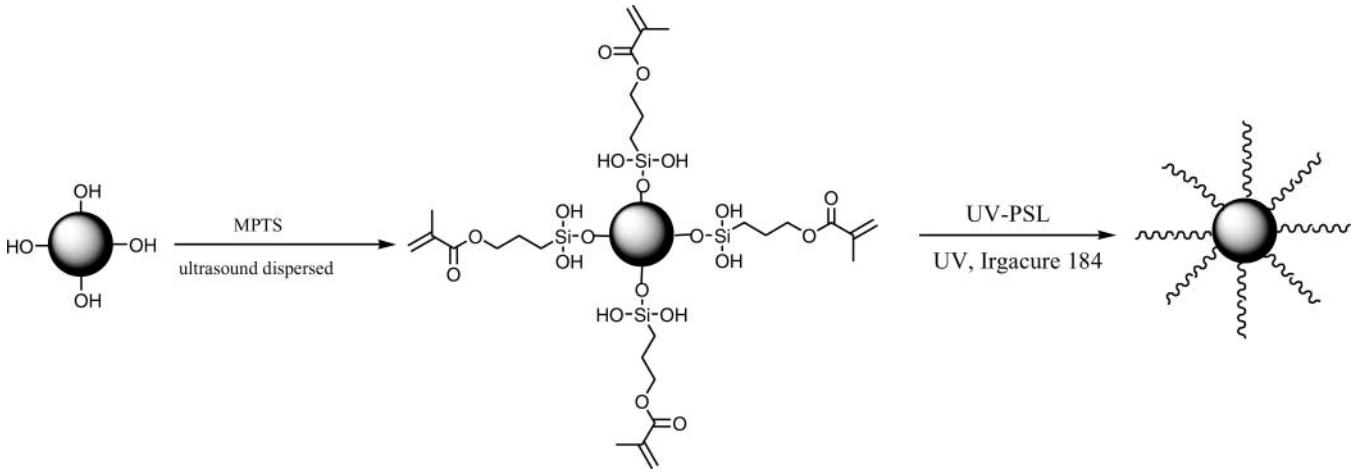

Sch. 1. The preparation of UV-cured silicone resin/silica nanocomposites.

nanocomposite formulations and FTIR, thermogravimetric (TG) and scanning electron microscopy (SEM) analyses were conducted on the free films prepared from the same coating formulations.

2 Experimental

2.1 Materials

The silica having mean particle size of 20 nm was kindly supplied by Aladdin Chemical Reagent Co., Ltd. 1-Hydroxycyclohexyl phenyl ketone (Irgacure 184), hydrochloric acid (HCl, 0.1 M), Phenyl trimethoxysilane (PTMS), methyl trimethoxysilane (MTMS) and 3-(methacryloxy) propyl trimethoxysilan (MPTS) were acquired from Aldrich Chemical Co., Ltd. Tinplate panels (75 mm × 150 mm × 0.82 mm) were used as substrates in all coating applications. All chemicals were of analytical grade and used without further purification. Doubly deionized water was used through all the processes.

2.2 Characterization

The FTIR measurements (Impact 400, Nicolet, Waltham, MA) were carried out with the KBr pellet method. Thermogravimetric results were obtained with a TA Instrument 2050 thermogravimetric analyzer at a heating rate of 10°C/min from 25 to 800°C under a nitrogen atmosphere. The morphology of the UV-cured nanocomposite films was examined using scanning electron microscopy (XL-20, Philips Corporation, Netherlands). Gel contents of the UV-cured films were determined by Soxhlet extraction for 6 h using acetone. Insoluble gel fraction was dried in vacuum oven at 40°C to constant weight and then the gel content was calculated. The coating properties were measured in accordance with the corresponding standard test methods as indicated. These include the thickness (ASTM D-1186), gloss (ASTM D-523-80), hardness (ASTM D3363), adhesion (ASTM D3359) and impact strength (ASTM D-2794-82).

2.3 Synthesis

2.3.1. *Surface Modification of Silica Particles*

Into a 250 mL dried round-bottom flask, 3.0 g nanosilica was ultrasound dispersed in 100 mL ethanol for 30 min, then 2.5 g MPTS was added and ultrasound dispersed for 2 h. The product was washed by centrifugations/redispersions three times in ethanol and dried in vacuum at room temperature for 24 h. The grafting density of grafted vinyl group was determined by TGA and was calculated by Equation 1 (28).

$$\text{Grafting density (mol/m}^2\text{)} = \frac{\left(\frac{W_{60-730}}{100-W_{60-730}}\right) \times 100 - W_{silica}}{MS_{spec} \times 100} \times 10^6 \quad (1)$$

where W_{60-730} is the weight loss from 60 to 730°C corresponding to the decomposition of the MPTS, M (g/mol) is the molar mass of the degradable part of the grafted molecule (205 g/mol), S_{spec} (m^2/g) and W_{silica} are the specific surface area and the weight loss of silica determined before grafting, respectively.

2.3.2. *Preparation of UV-curable Polysilisiquioxane*

The UV-curable polysilisiquioxane (UV-PSL) containing methacrylic groups was synthesized by an alternative sol-gel process according to a reported method (28). The mixture of PTMS, MTMS and MPTS combined with 0.1 M aqueous hydrogen chloride (pH=1.0) in a sealed container, was stirred for 2 h at 25°C (Sch. 2). The resulting sol was dissolved in an equal volume of ether and then washed by deionized water until pH was 6–7. The solvent was then removed under vacuum at 40°C and transparent liquid resins were obtained. The molar ratio of PTMS / MTMS / MPTS

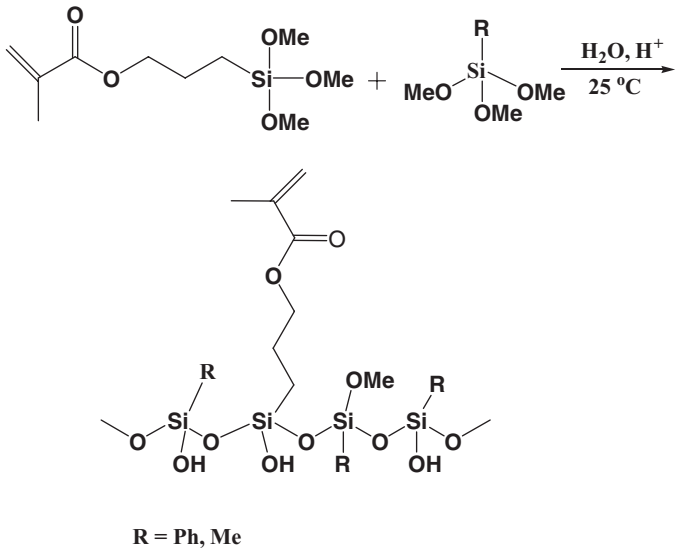

Sch. 2. Synthetic route of the UV-curable polysilisiquioxane.

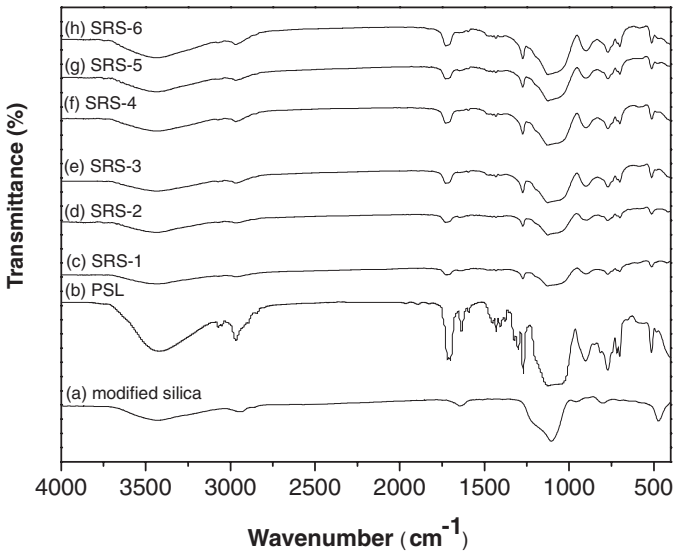

Fig. 1. FTIR spectra of (a) modified silica, (b) UV-PSL, (c-h) silicone resin/silica nanocomposites.

was 80/5/15 and molar ratio of water to methoxysilane was 1.2.

2.3.3. *Preparation of Silicone Resin/Silica Nanocomposites*

UV curable coating formulations were prepared by mixing the MPTS-modified silica particles, UV-PSL, and photoinitiator (Irgacure 184). Each formulation was prepared in a beaker with ultrasonic stirring for 1 h until they became clear and homogeneous. In order to remove air bubbles formed during mixing; the beaker content was kept under gentle vacuum for 20 min. After removal of air bubbles, the prepared formulations were applied onto tinplate panels using a wire gauged bar applicator in order to obtain uniform thickness of 30 μm. The applied wet coatings were cured by UV light ($\lambda_{max} = 365$ nm, power density approximately 20 mW/cm^2) situated 15 cm above tinplate panels for 180 s. The composition of coating formulations is given in Table 1.

Table 1. Compositions of the silicone resin/silica nanocomposites

Sample	*UV-PSL (g)*	*MPTS-modified silica (g)*	*Irgacure 184 (g)*
SRS-1	10	0	0.3
SRS-2	10	0.05	0.3
SRS-3	10	0.1	0.3
SRS-4	10	0.2	0.3
SRS-5	10	0.4	0.3
SRS-6	10	0.6	0.3

3 Results and Discussion

3.1 Analysis of FTIR

Figure 1 shows the FTIR analysis of (a) modified silica, (b) UV-PSL, (c-h) silicone resin/silica nanocomposites with 0–6 wt% modified silica content. As is clearly known, silane-coupling agents are often used to treat the silica particles due to their unique bifunctional structure with one end capable of reacting with the silanol groups on silica surface and the other end compatible with the polymer (29). Figure 1(a) shows the FTIR spectrum of methacrylic functional silica particles. From the characteristic C–H stretching band at 2840 and 2940 cm^{-1}, C=O stretching vibration at 1720 cm^{-1}, and C=C stretching mode at 1650 cm^{-1}, the existence of methacrylic groups on the particles has been proved. In addition, the strong Si–O–Si band can be seen at 1100 cm^{-1}.

In Figure1(b), the IR peaks of O–H stretching mode at 3420 cm^{-1}, and Si–O–Si asymmetric stretching modes at 1000–1180 cm^{-1} for polysiloxane existed, together with CH_3 peaks near 2970 and 1270 cm^{-1} for side chains of polysiloxane. In addition, the FTIR peaks of C=C (in methacrylate group) stretching mode at 1640 cm^{-1} and C=O stretching vibration at 1720 cm^{-1} existed. The methacrylate groups in resins make them photopatternable. Upon UV exposure and in the presence of the photoinitiator (Irgacure 184), a free radical polymerization could easily occur and most C=C reacted after 180 s as described in Figure 1(c-h). The IR peaks of C=O bond at 1720 cm^{-1} was shifted to a higher wavenumber after UV exposure because the C=O bond could not be conjugated further since the entire C=C double bonds in the polysilisiquioxane were mostly cross-linked by UV irradiation. As is shown in

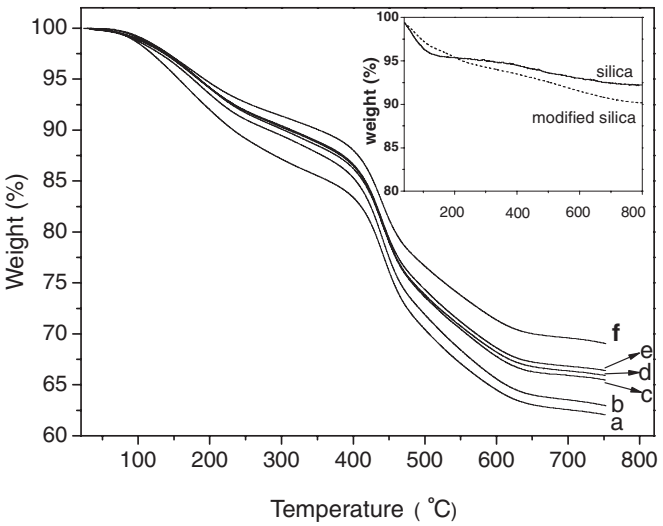

Fig. 2. TGA curves of nanosilica, MPTS-modified silica, and silicone resin/silica nanocomposites (a: SRS-1; b: SRS-2; c: SRS-3; d: SRS-4; e: SRS-5; f: SRS-6).

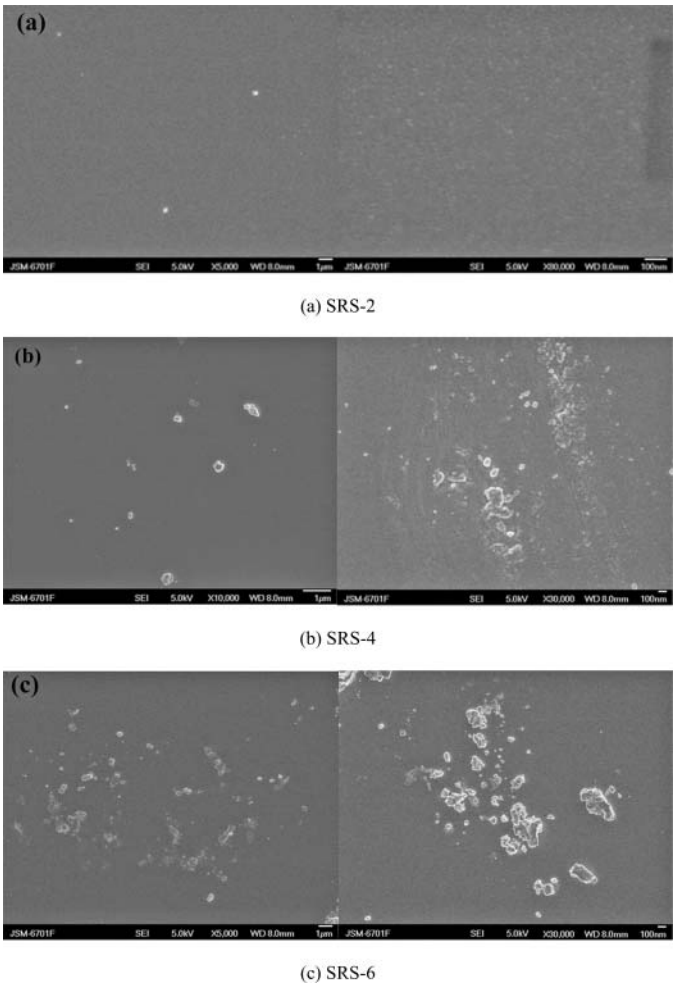

Fig. 3. SEM images of silicone resin/silica nanocomposites: (a) SRS-2, (b) SRS-4, and (c) SRS-6.

Figure 1(c-h), the Si—O—Si asymmetric stretching mode at 1000–1180 cm^{-1} was enhanced with the addition of modified silica particles.

3.2 Analysis by TGA

The bare silica and methacrylate-modified silica were investigated by TGA analysis. The high temperature required to decompose and evaporate the organic content of the modified silica particles demonstrates that the silane-coupling agent is strongly bound to the particle surface and one can expect a covalent bond (30). Calculation based on TGA shows that the grafting density of grafted vinyl group is 0.92 μmol/m^2 calculated from Equation 1.

The thermal properties of the nanocomposite coatings were characterized by TGA in nitrogen atmosphere. The TGA curves of pure silicone resin and in the presence of modified silica are shown in Figure 2. Silicone resin/silica nanocomposites showed a severe weight loss 2–4% from 25 to 130°C. This may be due to the release of bound moisture, which was through the formation of hydrogen bonds between the carbonyls or between the carbonyls and the hydroxyl groups present in the silicone resin. The second mass losses from about 150 to 350°C are attributed to dehydration of silanol groups present in the silicone resin and modified silica. A sharp loss in mass is observed at 400°C and continues to 600°C, possibly due to a large scale thermal degradation of the silicone resin. It is well known that silicone resin degrades to a volatile low-molecular weight cyclic siloxanes by a two-step process in nitrogen, and these two steps are "unzipping" reactions induced by silanol terminal groups and "random main chain scission" reactions, respectively. It can be seen from Figure 2 that the silicone resin/silica nanocomposites (Fig. 2(b-f)) lost weight more slowly during the TGA than did the pure silicone resin (Fig. 2(a)), indicating that the composites with better dispersed silica are more thermally stable and these can be attributed to the retardation effect of modified silica as barriers for the degradation of silicone resin. The residual weight is increased with the addition of modified silica.

3.3 Analysis of Morphology

Figure 3 summarizes the surface morphology of SEM images of silicone resin/silica nanocomposites containing different silica contents. It is clearly observed that these particles had a very small size and homogeneously distributed through the surface when the nanosilica content is low (Fig. 3(a, b)). In addition, the fractured surface morphology of SEM image of SRS-4 is shown in Figure 4. The SEM micrograph shows that particles dispersed uniformly throughout the matrix. However, when the silica content is increased to 6 wt%, some particles with a size of about 200 nm are visible

Table 2. Properties of nanocomposites

Sample	*Thickness (μm)*	*Gel content (%)*	*Adhesion*	*Gloss (85°)*	*Hardness*	*Impact strength (kg·cm)*
SRS-1	30	92	5B	99.2	6H	50
SRS-2	30	94	5B	98.9	6H	50
SRS-3	31	93	5B	98.5	6H	50
SRS-4	30	94	5B	97.9	6H	50
SRS-5	28	94	5B	96.1	6H	50
SRS-6	30	95	5B	94.6	6H	50

on the surface (Fig. 3(c)). These particles should be part of the large silica aggregates. The larger particle size could be explained on the basis of surface modification. It is possible that the beads become joined as a result of the surface modification process. The particles approaching each other may be crosslinked by the reaction of the surface silanol groups or by the reaction of one MPTS molecule with different silica particles.

3.4 Analysis of Properties of Nanocomposites

In order to evaluate the UV-curable properties of the nanocomposites, each formulation was applied onto tinplate panels using an applicator and exposed to UV light (λ_{max} = 365 nm, power density approximately 20 mW·cm^{-2}) for 180 s. After the UV exposure, the sample was cured in the convection oven at 200°C for 2 h. The coated tinplate panels were subjected to performance tests and the results are listed in Table 2. Each result reported is an average of four separate measurements performed. The crosscut adhesion experiments showed that 100% adhesion was reached for all coating compositions. Impact strength of all nanocomposite coatings is high. Dropping 1 kg weight over 50 cm, no damage could be seen on coatings. Good adhesion is important for this test. As can be seen in Table 2, the gloss of nanocomposite coatings decreased slightly with increasing silica because the refractive index of silica nanoparticles was different from that of silicone resin. However we can say that between these values there is no sharp difference. The hardness of the films was measured. All nanocomposite films exhibited excellent hardness as high as 6H. This would indicate that nanocomposite coatings tend to be hard.

Moreover, gel contents of the modified silica containing nanocomposite films are reported in Table 2. The data indicate the formation of an almost complete insoluble crosslinked network (gel content values always above 90%).

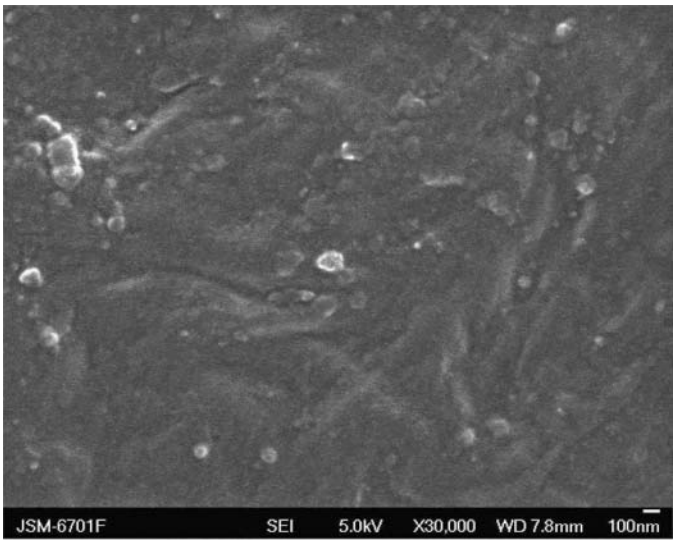

Fig. 4. SEM image of the fractured surface of SRS-4.

4 Conclusions

In this paper, a series of UV curable nanocomposites containing MPTS-modified silica particles, UV-PSL, and photoinitiator was prepared. SEM studies indicate that the modified silica particles were dispersed homogenously through the silicone resin. MPTS acts as a coupling agent between silica particles and the polymer matrix. The thermal stability (by TGA) of nanocomposites was slightly enhanced with the addition of silica particles. The nanocomposite films exhibited significant enhancement in mechanical properties including hardness and adhesion.

References

1. Goettler, L.A., Lee, K.Y. and Thakkar, H. (2007) *Polym. Rev.*, 47(2), 291–317.
2. Choudalakis, G. and Gotsis, A.D. (2009) *Eur. Polym. J.*, 45(4), 967–984.
3. Kickelbick, G. (2003) *Prog. Polym. Sci.*, 28(1), 83–114.
4. Sumita, M., Tsukurmo, T., Miyasaka, K. and Ishikawa, K. (1983) *J. Mater. Sci.*, 18(6), 1758–1764.
5. Zhang, S.W., Zhou, S.X., Weng, Y.M. and Wu, L.M. (2005) *Langmuir*, 21(6), 2124–2128.
6. Zan, L., Fa, W. and Wang, S. (2006) *Environ. Sci. Technol.*, 40(5), 1681–1685.
7. Li, Y.Q., Yang, Y., Fu, S.Y., Yi, X.Y., Wang, L.C. and Chen, H.D. (2008) *J. Phys. Chem. C.*, 112(47), 18616–18622.
8. Corr, S.A., Rakovich, Y.P. and Gun'Ko, Y.K. (2008) *Nanoscale Res. Lett.*, 3(3), 87–104.
9. Verónica, S.M. and Miguel A, C.D. (2007) *Advan. Mater.*, 19(23), 4131–4144.
10. Pyun, J. (2007) *Polym. Rev.*, 47(2), 231–263.

11. Çelıİk, M. and Önal, M. (2006) *J. Macromol. Sci. Part A-Pure Appl. Chem.*, 43(6), 933–943.
12. Coltrain, B.K., Landry, C.J.T., O'Reilly, J.M., Chamberlain, A.M., Rakes, G.A., Sedita, J.S., Kelts, L.W., Landry, M.R. and Long, V.K. (1993) *Chem. Mater.*, 5(10), 1445–1455.
13. Wenning, A. (2002) *Macromol. Symp.*, 187(1), 597–604.
14. Kim, Y.B., Park, J.M., Kim, H.K. and Hong, J.W. (2001) *Polym. Bull.*, 47(3–4), 313–319.
15. Soppera, O. and Croutxe, B.C. (2003) *J. Polym. Sci. Part A-Polym. Chem.*, 41(5), 716–724.
16. Decker, C. (1998) *Polym. Int.,* 45(2), 133–141.
17. Vollath, D. and Szabo, D.V. (2004) *Adv. Eng. Mater.*, 6(3), 117–127.
18. Uhl, F.M., Davuluri, S.P., Wong, S.C. and Webster, D.C. (2004) *Chem. Mater.*, 16(6), 1135–1142.
19. Decker, C., Zahouily, K., Keller, L., Benfarhi, S., Bendaikha, T. and Baron, J. (2002) *J. Mater. Sci.*, 37(22), 4831–4838.
20. Benfarhi, S., Decker, C., Keller, L. and Zahouily, K. (2004) *Eur. Polym. J.*, 40(3), 493–501.
21. Tan, H. and Nie, J. (2007) *Macromol. React. Eng.*, 1(3), 384–390.
22. Sangermano, M., Malucelli, G., Amerio, E., Priola, A., Billi, E. and Rizza, G. (2005) *Progr. Org. Coat.*, 54(2), 134–138.
23. Li, F., Zhou, S. and Wu, L. (2005) *J. Appl. Polym. Sci.*, 98(3), 1119–1124.
24. Wang, T. and Wang, Z.H. (2005) *Polym. Bull.*, 53(5–6), 323–331.
25. İnan, T.Y., Ekinci, E., Kuyulu, A. and Güngör, A. (2002) *Polym. Bull.*, 47(5), 437–444.
26. Wang, H., Mei, M., Jiang, Y., Li, A., Zhang, X. and Wu, S. (2002) *Polym. Int.*, 51(1), 7–11.
27. Bartholome, C., Beyou, E., Bourgeat-Lami, E., Chaumont, P. and Zydowicz, N. (2003) *Macromolecules*, 36(21), 7946–7952.
28. Zhang, H., Wang, J., Li, L., Song, Y., Zhao, M. and Jian, X. (2008) *Thin Solid Films*, 517(2), 857–862.
29. Sun, Y., Zhang, Z. and Wong, C.P. (2005) *J. Colloid Interface Sci.*, 292(2), 436–444.
30. Hartwig, A., Sebald, M. and Kleemier, M. (2005) *Polymer*, 46(7), 2029–2039.